Published in final edited form as:
Opt Lett. 2010 November 15; 35(22): 3838–3840.

Microlens array recording of localized retinal responses

Qiu-Xiang Zhang[1], **Jin-Yu Wang**[1], **Lei Liu**[2], and **Xin-Cheng Yao**[1,*]

[1]Department of Biomedical Engineering, University of Alabama at Birmingham, Birmingham, AL 35294

[2]Department of Optometry, University of Alabama at Birmingham, Birmingham, AL 35294

Abstract

A rapid functional imager was designed for parallel recording of localized intrinsic optical signals (IOSs). This imager used a microlens array (MLA) based illuminator to deliver visible stimulus light and near infrared recording light simultaneously. The parfocal configuration of the stimulus and recording light illumination enabled confocal recording of stimulus-evoked IOSs. Because the MLA stimulation/recording spots were widely separated on the retina, and only photoreceptors within MLA stimulation/recording spots were stimulated, the potential IOS cross-talk effect among neighboring retinal areas was minimized. Our experiments revealed robust IOS activities tightly correlated with localized retinal responses.

The purpose of this study is to demonstrate the feasibility of simultaneously recording stimulus-evoked intrinsic optical signals (IOSs) from multiple retinal locations. Fast IOS recording of localized retinal responses may be useful in functional evaluation of retinal neural damage associated with eye diseases, such as cone-rod dystrophy, age-related macular degeneration (AMD), and retinitis pigmentosa (RP).

Electrophysiological measurements, such as electroretinogram (ERG), are valuable for objective assessment of retinal dysfunctions. ERG a- and b-waves are often taken as the functional indices of photoreceptors and post-photoreceptor neurons, respectively. However, ERG integrates stimulus-evoked electrophysiological responses over an extended retinal area, the effects of localized small lesions associated with early retinal diseases may be concealed by spatial integration.

IOS imaging holds promise for high resolution assessment of retinal neural functions. Several imaging techniques, such as fundus cameras [1-3], adaptive optics ophthalmoscopes [4-6], optical coherence tomography (OCT) imagers [7-10] have been used to demonstrate the feasibility of IOS imaging of retinal activation. Using isolated amphibian retinas, high-spatial (μm) and high-temporal (ms) imaging revealed spatially intermixed positive (increasing) and negative (decreasing) IOS signals [11,12]. Unless the imaging resolution is high enough, the IOSs of opposite polarities may be integrated spatially and result in poor imaging signal sensitivity. While both confocal [13] and optical coherence tomography (OCT) [7-9] systems can provide the high spatial resolution to map IOSs in the retina, signal contaminations among adjacent retinal volumes may still exist because stimulus-evoked light dynamics of neighboring volumes, such as transient transmission and scattering changes, may produce dynamic change of the photons collected from the intended sampling

*Corresponding author: xcy@uab.edu.

OCIS codes: 170.2655 Functional monitoring and imaging; 330.4270 Vision system neurophysiology; 330.5310 Vision . photoreceptors.

volumes. In order to detect localized retinal response without significant contaminations from neighboring retinal volumes, we developed a MLA-based functional imager.

The schematic diagram of the MLA-based imager is shown in Fig. 1a. In this system, a NIR (center wavelength: 830 nm; bandwidth: 60 nm) superluminescent laser diode (SLD) (SLD-35-HP, Superlum) was used for IOS imaging, a NIR (850 nm) light-emitting diode (LED) was used to examine the MLA spots on the retina, and a red (635 nm) laser diode was used for retinal stimulation. At the dichroic mirror (DM), collimated NIR light and visible light were combined to illuminate the MLA (MLA-0200-1.0-S, Adaptive Optics Associates), and thus simultaneously produced the MLA visible stimulation light and NIR recording light patterns on the back focal plane of the MLA. The MLA spot pattern was coincided with the front focal plane of the lens L1 (f = 80mm), and thus the MLA patterns could be relayed to the specimen (retina) at the back focal plane of the objective (f = 18mm, 10X/0.3), with a demagnification of 0.225 (i.e., 18 mm/80 mm). The pitch of the MLA was 200 μm, and the spacing of the spots on the retinal sample was 45 μm. The back focal plane of the lens L1 coincided with the incident aperture of the objective, and thus the numeric aperture (NA) of the objective could be fully used to produce optimized (i.e., sharpest and minimized) light foci. Using a 10X/0.3 objective, this MLA-based system, in theory, could achieve a transversal resolution ($0.61\lambda/NA$) of ~1.7 μm and axial resolution (λ/NA^2) of ~9.2 μm. In order to minimize the optical dispersions between the NIR illumination light and visible stimulus light, achromatic lenses were used in the system shown in Fig. 1(a) (i.e. L1, L2). The MLA associated dispersions should also be considered. In theory, the chromatic aberration of the NIR (830nm) and red light at the specimen (retina) produced by the MLA is ~2.1 μm, which is negligible compared to the axial resolution (9.2 μm) of the system. Therefore, the confocal configuration of the NIR illumination and red stimulation light foci was feasible to realize localized multiple spots measurement of stimulus-evoked IOSs with cellular resolution in both transversal and axial directions.

A polarization-sensitive beam splitter (PBS, G335-599000, Linos) was employed to ensure the high efficiency of the NIR imaging light. Linear s-polarized NIR light was reflected into the specimen (retina) by the PBS. Between the PBS and the objective, a quarter-wave ($\lambda/4$) retarder, with fast axis at 45° relative to the polarization plane of the illumination light, converted the linear-polarized (s-state) light to circular-polarized. For the reflected light from the specimen, it would be p-polarized after a double-passing through the quarter-wave plate, and thus could fully transmit through the PBS into the imaging path. A CCD camera (Pike F-032B/C, Allied Vision Technologies) working in a high speed mode (3ms/frame, i.e., 333 Hz) was used for retinal imaging.

Flat-mounted, isolated leopard frog (Rana Pipiens) retinas were used in the experiments. Briefly, retinal dissection was conducted in a dark room with dim red illumination [14]. After dark adaptation, the frog was euthanized by rapid decapitation and double pithing before the eyes were enucleated. The eyeball was hemisected below the equator with a pair of fine scissors to remove the lens and anterior structures before separating the retina from the retinal pigment epithelium. The dissection of the retina was performed in Ringer's solution containing (in mM) [15]: 110 NaCl, 2.5 KCl, 1.6 MgCl2, 1.0 CaCl2, 22 NaHCO3, and 10 D-glucose. During the experiment, the flat-mounted retina was immersed in the Ringer's solution. In principle, the MLA recording system can simultaneously monitor 13 × 9 retinal foci (i.e., 640 × 480 CCD pixels) with a focal distance of 45 μm at the specimen. However, in order to improve the IOS imaging speed, a reduced image area (300 × 300 CCD pixels) was used to monitor 6 × 6 retinal locations. Fig.1b shows the MLA pattern by placing a mirror at the specimen plane. When the retina was imaged, the MLA pattern was a little blurred due to the light scattering in the retina. However, the MLA spots were still distinguishable (Fig. 1c), and the cross-talk noise among adjacent spots were negligible.

Before IOS recording, the NIR LED was turned on to confirm that the MLA was focused at the photoreceptor layer (Fig. 1d). During the IOS recording, the NIR LED for transmission imaging was turned off. In each imaging session, pre-stimulus baseline recording was collected for 1.2 s (i.e., 400 frames) before the 1-s visible red light stimulus was delivered.

Both positive and negative IOS signals were observed around each MLA spot (Fig. 2). Rapid IOS responses occurred almost immediately after the stimulus onset (Fig. 2g). The amplitude peaks of localized positive (such as the signal represented by trace 3 in Fig. 2(c)) and negative (such as the signal represented by trace 8) IOSs could be as large as 40% ΔI/I, where ΔI was the dynamic optical changes and I was the average pre-stimulus background pixel value (light intensity). Previous studies with isolated photoreceptor outer segments and isolated retinas have demonstrated transient IOSs associated with phototransduction [16-18]. Both binding and release of G-proteins to photoexcited rhodopsin might contribute to the IOSs [17]. Localized IOSs at different MLA recording spots had slightly different signal distributions, time courses and signal amplitudes (Fig. 2b and 2c), but the averages of overall positive and negative signals appeared to have similar time courses (Fig. 2d). Because of the comparable time courses of the overall positive and negative signals, the IOS magnitude, i.e., absolute value $|IOS|$, can be used as the single parameter to quantify the strength of localized photoreceptor activity (Fig. 2e). In order to minimize the effect of spatial variations, including MLA spot locations relative to localized photoreceptors, on each MLA recording location, we recorded additional 5 image sequences on the same specimen by shifting the sample platform in the same direction for 2, 4, 6, 8 and 10 μm, respectively, in transversal direction; with the MLA illumination consistently focused on the photoreceptor layer. Fig. 2f represents the averaged IOS magnitude pattern of these 6 recording trials. In Fig. 2f, a relatively homogenous IOS pattern was observed (compared to single-trial recording shown in Fig. 2e), and all MLA recoding spots revealed robust IOSs with a magnitude up to 15% ΔI/I. Fig. 2g shows temporal dynamics of the averaged IOS activity, and confirms that rapid IOS occurred almost immediately after the stimulus onset.

In summary, we demonstrated that a high-speed MLA-based imager can simultaneously record stimulus-evoked IOSs from multiple retinal locations in flat-mounted frog retinas that were associated with localized neural responses to visible light stimulation. In this recording system, the MLA provided the visible stimulus light and the near infrared recording light simultaneously. Because only the photoreceptors within the stimulus/recording locations were activated, the IOS cross-talk effect from adjacent photoreceptors and post-photoreceptor neurons were reduced (compared to full-field illumination/recording system). Localized IOS responses with magnitude peaks up to 40% ΔI/I were consistently observed (Fig. 2). Because both the visible stimulus and the NIR recording light were focused at the photoreceptor layer, and because of the very short IOS delay after stimulus onset, we believe that the observed IOSs resulted primarily from the activities of the photoreceptors. Moreover, the MLA-based imager can evaluate multiple locations over an extended retinal region simultaneously, producing an accurate retinotopic function map in one image sequence. This recording method avoids assembling measurements taken from different time frames, and thus is much less vulnerable to inevitable eye movements. In the future development of IOS-based clinical ophthalmic devices, the ability of parallel recording of multiple retinal loci can be a great advantage over other retinal function evaluation modalities, such as visual field or multi-focal ERG. We anticipate that further experimentation on the properties of the visible light stimulus, such as its temporal modulation, spatial layout, color and intensity will allow selective evaluation of the rod and cone systems. Accurate assessment of localized retinal rod and/or cone photoreceptor dysfunctions will lead to early detection and improved treatment evaluation of the eye diseases such as cone-rod dystrophy, AMD, RP, that are known to produce pathological changes in the retinal photoreceptors in their early stage.

Acknowledgments

This research is supported by Dana Foundation (Brain and Immuno-Imaging Grant Program), Eyesight Foundation of Alabama, and NIH (1R21RR025788-01).

Reference

1. Schallek J, Li H, Kardon R, Kwon Y, Abramoff M, Soliz P, Ts'o D. Stimulus-evoked intrinsic optical signals in the retina: spatial and temporal characteristics. Invest Ophthalmol Vis Sci 2009;50:4865–4872. [PubMed: 19420337]
2. Hanazono G, Tsunoda K, Shinoda K, Tsubota K, Miyake Y, Tanifuji M. Intrinsic signal imaging in macaque retina reveals different types of flash-induced light reflectance changes of different origins. Invest Ophthalmol Vis Sci 2007;48:2903–2912. [PubMed: 17525227]
3. Okawa Y, Fujikado T, Miyoshi T, Sawai H, Kusaka S, Mihashi T, Hirohara Y, Tano Y. Optical imaging to evaluate retinal activation by electrical currents using suprachoroidal-transretinal stimulation. Invest Ophthalmol Vis Sci 2007;48:4777–4784. [PubMed: 17898304]
4. Jonnal RS, Rha J, Zhang Y, Cense B, Gao WH, Miller DT. In vivo functional imaging of human cone photoreceptors. Opt Express 2007;15:16141–16160.
5. Grieve K, Roorda A. Intrinsic signals from human cone photoreceptors. Invest Ophthalmol Vis Sci 2008;49:713–719. [PubMed: 18235019]
6. Rha J, Schroeder B, Godara P, Carroll J. Variable optical activation of human cone photoreceptors visualized using a short coherence light source. Optics letters 2009;34:3782–3784. [PubMed: 20016612]
7. Yao XC, Yamauchi A, Perry B, George JS. Rapid optical coherence tomography and recording functional scattering changes from activated frog retina. Applied Optics 2005;44:2019–2023. [PubMed: 15835350]
8. Bizheva K, Pflug R, Hermann B, Povazay B, Sattmann H, Qiu P, Anger E, Reitsamer H, Popov S, Taylor JR, Unterhuber A, Ahnelt P, Drexler W. Optophysiology: depth-resolved probing of retinal physiology with functional ultrahigh-resolution optical coherence tomography. Proceedings of the National Academy of Sciences of the United States of America 2006;103:5066–5071. [PubMed: 16551749]
9. Srinivasan VJ, Wojtkowski M, Fujimoto JG, Duker JS. In vivo measurement of retinal physiology with high-speed ultrahigh-resolution optical coherence tomography. Opt Lett 2006;31:2308–2310. [PubMed: 16832468]
10. Schmoll T, Kolbitsch C, Leitgeb RA. In vivo functional retinal optical coherence tomography. Journal of Biomedical Optics 2010;15
11. Li YC, Strang C, Amthor FR, Liu L, Li YG, Zhang QX, Keyser K, Yao XC. Parallel optical monitoring of visual signal propagation from the photoreceptors to the inner retina layers. Optics letters 2010;35:1810–1812. [PubMed: 20517424]
12. Yao XC, Zhao YB. Optical dissection of stimulus-evoked retinal activation. Optics Express 2008;16:12446–12459. [PubMed: 18711481]
13. Li YG, Liu L, Amthor F, Yao XC. High-speed line-scan confocal imaging of stimulus-evoked intrinsic optical signals in the retina. Optics letters 2010;35:426–428. [PubMed: 20125743]
14. Yao XC, Zhao YB. Optical dissection of stimulus-evoked retinal activation. Opt Express 2008;16:12446–12459. [PubMed: 18711481]
15. Sieving PA, Murayama K, Naarendorp F. Push-pull model of the primate photopic electroretinogram: a role for hyperpolarizing neurons in shaping the b-wave. Vis Neurosci 1994;11:519–532. [PubMed: 8038126]
16. Hofmann KP, Uhl R, Hoffmann W, Kreutz W. Measurements on fast light-induced light-scattering and -absorption changes in outer segments of vertebrate light sensitive rod cells. Biophys Struct Mech 1976;2:61–77. [PubMed: 963228]
17. Kuhn H, Bennett N, Michel-Villaz M, Chabre M. Interactions between photoexcited rhodopsin and GTP-binding protein: kinetic and stoichiometric analyses from light-scattering changes.

Proceedings of the National Academy of Sciences of the United States of America 1981;78:6873–6877. [PubMed: 6273893]

18. Arshavsky VY, Lamb TD, Pugh EN Jr. G proteins and phototransduction. Annual review of physiology 2002;64:153–187.

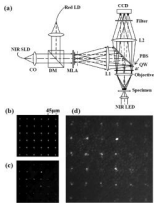

Fig.1.

(a) Schematic diagram of the MLA recording system: CO, collimator; DM, dichroic mirror; MLA, microlens array; PBS, polarization-sensitive beam splitter; QW, quarter-wave plate. Focal lengths of the lenses L1 and L2 are 80 and 150 mm, respectively. NIR SLD was used for IOS imaging. Red laser diode (LD) was used for retinal stimulation. NIR LED was used for transmission imaging of the retina. At the dichroic mirror (DM), collimated NIR recording light and visible stimulus light were combined together to illuminate microlens array (MLA) simultaneously. (b) Representative MLA pattern by placing a mirror at the specimen plane. (c) Representative MLA imaging pattern of an isolated frog retina. (d) Simultaneous MLA recording and transmission imaging of the retina.

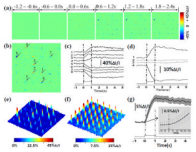

Fig.2.

(a) MLA recording of retinal activation. Each illustrated IOS image is an average over 600 ms interval (i.e., 200 frames, 3 ms/frame). (b) Enlargement of the 4th frame in (a). (c) Black traces 1-8 show IOSs of randomly selected 8 pixels pointed by the arrowheads in (b). (d) Black traces 1 and 4 show the average of all the positive and negative IOSs within the MLA spot areas. Gray traces 2 and 3 show the positive and negative IOSs without stimulus. (e) IOS magnitude map of the single-trial MLA recording shown in (b). (f) Averaged IOS magnitude map of 6 MLA recordings. (g) Temporal dynamics of overall IOS magnitude shown in (f).